TU Delft

Delft University of Technology

Document Version
Final published version

Citation (APA)
Gunawardena, K. R. A., Maiullari, D., & van Esch, M. M. E. (2026). *Enhancing the climate resilience of Amsterdam quays: Simulating urban tree contributions*. Paper presented at 38th PLEA conference Costa Rica 2026, San Jose, Costa Rica. https://doi.org/10.5281/zenodo.21823870

Important note
To cite this publication, please use the final published version (if applicable).
Please check the document version above.

Copyright
In case the licence states “Dutch Copyright Act (Article 25fa)”, this publication was made available Green Open Access via the TU Delft Institutional Repository pursuant to Dutch Copyright Act (Article 25fa, the Taverne amendment). This provision does not affect copyright ownership.
Unless copyright is transferred by contract or statute, it remains with the copyright holder.

Sharing and reuse
Other than for strictly personal use, it is not permitted to download, forward or distribute the text or part of it, without the consent of the author(s) and/or copyright holder(s), unless the work is under an open content license such as Creative Commons.

Takedown policy
Please contact us and provide details if you believe this document breaches copyrights.
We will remove access to the work immediately and investigate your claim.

This work is downloaded from Delft University of Technology.

PLEA 2026 – COSTA RICA
Common Sense Architecture – Harnessing Local Wisdom for Sustainable Future

Enhancing the climate resilience of Amsterdam quays:
Simulating urban tree contributions

KANCHANE GUNAWARDENA[1], DANIELA MAIULLARI[1], MARJOLEIN VAN ESCH[1]

[1] Delft University of Technology, Delft, Netherlands.

1 INTRODUCTION

As increased urbanisation places greater demands on urban infrastructure, the need to ensure reliable performance and resilience to future risks becomes a critical consideration for municipalities. The city of Amsterdam is no exception, with the atypical inclusion of an extensive engineered canal network serving its essential infrastructural needs. This infrastructural asset is however in many parts dated and strained by increasing demands, including climate resilience. Thus, there is an urgent necessity to restore and improve this asset to deliver expected current and future performance, including resilience to climate warming challenges such as safeguarding pedestrian thermal comfort to support urban walkability [1].

The *Multifunctional Quay Walls* project re-imagines traditional Amsterdam quays as multifunctional systems that enhances climate adaptation, biodiversity, circularity, and sustainable logistics, while respecting its heritage value. Addressing the urgent need for life-extending interventions for ageing quay walls and bridges, the project prioritises renovation over replacement, while combining iterative design research methodologies with quantitative environmental modelling and simulation to generate and assess proposals for implementation.

This conference paper focuses on a part of this broader project, which considers green infrastructure enhancements principally represented by tree planting to maximise their widely supported potential to mitigate ever-worsening heat-related risks to urban pedestrians [2–4]. The body of work utilises simulation-based analyses of narrow bed canal configurations (typical canal width ~15 m, and each quay/bank width ~6 m), one of the two common typologies identified in Amsterdam.

The simulation studies evaluated under current climate conditions for a warm and hot day aims at quantifying the benefits of tree integration along such narrow bed canal banks. Scenario-based simulations include variations in linear spacing and tree age to assess contributions to thermal stress mitigation, resulting from differences in shading and evapotranspiration influence.



Figure 1. Egelantiersgracht Canal, Amsterdam (narrow bed).

2 METHODOLOGY

This study uses a simulation-based approach to evaluate changes in urban microclimates and associated thermal comfort owing to tree arrangements. The methodology combines Geographic Information System (GIS) data processing with three-dimensional microclimate modelling using ENVI-met (v5.9), a widely validated tool for urban microclimate studies [5–7].

First, the study area from the Amsterdam UNESCO heritage zone was delineated based on the presence of typical narrow canal beds and adjacent urban morphology. High-resolution GIS datasets, including building footprints, canal geometry, land surface cover, and digital elevation models were collected and processed. The data was then imported into ENVI-met's modelling environment to construct the representation of current conditions at 1 m^3 resolution. Static variables including building heights, surface materials, and canal waterbodies were parameterised using data from the Amsterdam Municipality (PDOK datasets) and field observations, as well as literature-based thermal property definitions. Subsequently, idealised derivative scenarios were developed to explore the impact of tree integration along canal banks.

Tree species definition was governed by Amsterdam's tree profile, with *Ulmus* spp. presenting notable dominance owing to their resilience to urban pollution and brackish waters and subsoil, as well as historical and heritage significance. The constrained root zones and canopy spread, and their biophysical characteristics, such as height, crown diameter, leaf area index (LAI), and transpiration rates, were approximated using ENVI-met's *Albero* database and derived variants (i.e., Quantitative Structure Model algorithm trees modified by scaling) [8].

Forcing data was obtained from the Royal Netherlands Meteorological Institute (KNMI), Schiphol (Station 240) 2025 Dataset, for a representative summer *warm day* (corresponding to validation data gathered for a cloud-free day), and a *hot day* to define the meteorological boundary conditions for the simulations, Table 1 [5–6].

Table 1: Meteorological boundary conditions for simulations.

Warm day rank	Date (2025)	Max T_a time	Max T_a (°C)	Shortwave radiation (W/m²)	Sunrise (CEST, UTC+2)	Sunset (CEST, UTC+2)
#45	25-Aug	17:00	23.2	~330.6	06:30	20:30
#01	01-Jul	16:30	35.45	~295	05:24	22:04

2.1 Model calibration and validation

The model environment and configuration of the present state were calibrated with reference to field data observations gathered at a representative narrow bed site on 25 August 2025. These observations were collected at Egelantiersgracht (see Figure 1), with established protocols implemented for summertime monitoring, including a cloud-free (6-hour) measurement period [9].

Table 2: Validation (VAL) case descriptions.

VAL case	Description	Forcing / wind handling	Period (#hrs)
VAL00	Kestrel-8, error corrected monitoring data (30-minute, mean)	Not forced	7
VAL01	KNMI Schiphol (unmodified)	All *Full*	7
VAL02	KNMI Schiphol (unmodified)	All *Full*	48
VAL03	KNMI Schiphol, WS & WD averaged between 25-Aug, 10:30 & 16:30 window	*Simple:* Wind *Full*: Others	7
VAL04	KNMI Schiphol, WS & WD averaged between 24 & 25-Aug	*Simple:* Wind *Full*: Others	48
VAL05	KNMI Schiphol, WS & WD Savitzky-Golay smoothed (***W1***)	All *Full*	7
VAL05a	KNMI Schiphol for 2025 - WS min & max clamped + WS & WD Savitzky-Golay smoothed (***W2***)	All *Full*	7
VAL05b	KNMI Schiphol for 2025 - WS min & max clamped + WS & WD Savitzky-Golay smoothed (***W2***)	All *Full*	16
VAL05c	KNMI Schiphol for 2025 - WS min & max clamped + WS & WD Savitzky-Golay smoothed (***W2***)	All *Full*	24
VAL05d	KNMI Schiphol for 2025 - WS min & max clamped + WS & WD Savitzky-Golay smoothed (***W2c***)	All *Full*	48

The observation data was then compared against the Egelantiersgracht site modelled and simulated for the same period in ENVI-met. Several validation cases (VAL) were considered to determine the best approach for the succeeding study (see Table 2). These VAL cases evaluated the following simulation configurations:

(a) Aggregation of ENVI-met 10-minute resolution output to 30-minute intervals, using either mean or median calculation (*VAL00*: 30-minute, mean-based).

(b) Given the acknowledged difficulties in using full wind forcing to sustain stable flow in ENVI-met, the influence of a signal smoothing approach applied to maintain flow deviations within permissible velocity (WS) and directional (WD) limits (see Table 3).

(c) The effect of priming / spin-up / warming-up simulation runs by up to 48-hours.

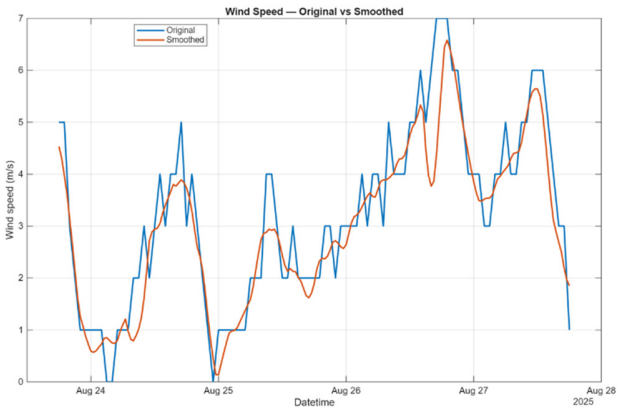


Figure 2. Wind signal smoothing (V_a: velocity signal).

The wind data 'smoothing' referred to under configuration option (b), describes the application of a workflow to suppress high-frequency noise while preserving the shape and amplitudes of slower trends and peaks of a uniformly sampled time series. The filter application considered Savitzky-Golay (SG) as the primary smoother with polynomial order p = *PolyOrder*, and frame length N= *FrameLength_samples* [10]. As a fallback when SG assumptions are not met, a moving-average (boxcar) filter with the same window length N is applied. Both p and N, and 'clamping' (capping WS to min. and max. values prior to smoothing), are settings that require refinement to ensure that a sampled duration presents a signal that ENVI-met can force without resulting in numerical instability and blowout. An example of a smoothed WS signal is presented in Figure 2; while for the complete smoothing methodology refer to supplementary statement: [11].

All VAL case results were assessed with reference to Willmott's d-index of agreement as the principal metric (and RMSE as a secondary) [12]. For Air Temperature (T_a) and Wind Speed (V_a), an agreement benchmark value of 0.7, and for Mean Radiant Temperature (T_{mrt}), a minimum acceptable benchmark of 0.5, was applied [13].

Table 3: Assessed wind 'smoothing' options (VAL05 family).

Weather files	Period (2025)	Method description	Settings used and notes
Weather File ***W1***	25-Aug (average warm day)	Savitzky-Golay smoothing of WS & WD only	Standard smoothing of WS and WD; no min/max clamps used.
Weather File ***W2***	24-25 Aug	WS min. & max. clamping + SG smoothing	Min. WS = 1 m·s^{-1}; Max. WS = 8 m·s^{-1}; (default scenario)
Weather File ***W2c***	24-25 Aug *(variant of W2)*	As above, with reduced p over a pre-window to smooth transitions	Min. WS = 2 m·s^{-1}; Max. WS = 7 m·s^{-1}; p = 2→1 from Aug-23 18:00 to Aug-25 03:00
Weather File ***W3***	01-Jul (warmest day)	WS min. & max. clamping + SG smoothing	Min. WS = 2 m·s^{-1}; Max. WS = 7 m·s^{-1}; N = 9 → 12.

2.2 Tree integration studies

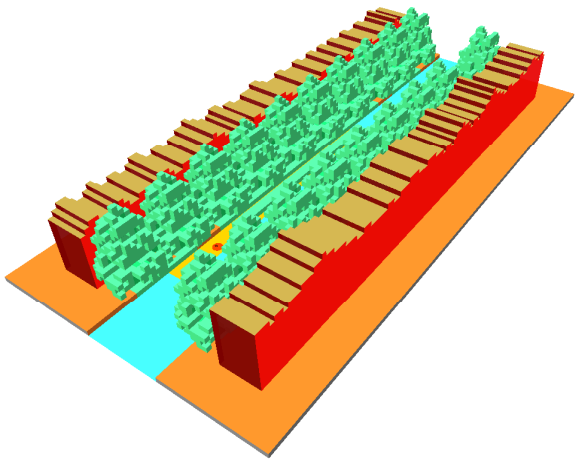


Figure 3. Idealised narrow canal in ENVI-met environment.

Using the observed narrow bed Egelantiersgracht canal as the foundation, idealised derivative scenario groups were developed (see Figure 4). The 'idealising' here refers to the isolation from the Egelantiersgracht site a linear, uniform 100 m length/segment of the canal including averaged building morphological and representative material characteristics. This in turn enables the presenting and interpretation of generalisable results.

ID0 represents the idealised 100 m canal canyon, oriented North-South, with East → West solar tracking, and excluding greening and trees (i.e., 'grey canyon' from which subsequent ID1 and ID2 tree integration scenario groups have been constructed.

ID1 scenario group considers linear elm tree spacing variation. Trunk centre-to-centre spacing is addressed by Municipality of Amsterdam guidance and historical references (Puccini Guide). These were reviewed as part of the broader project, considering minimum rootable volume (25 m^3), belowground servicing, and intended quay reconstruction methods. Following the review, a trunk centre-to-centre range between 7 m (historical minimum) and 15 m was recommended for the simulation-based study (i.e., #9 scenarios). For this ID1 scenario group, a fixed tree 'Age Class' of *Old-1* (Amsterdam UNESCO heritage zone elm population frequency rank #1) was applied as the expected/designed mature tree canopy.

ID2 scenario group considers canopy extent influence, by using elm tree age as a proxy. The relevant ENVI-met *Albero* representations of elm age classes were developed with reference to a regression growth model, established in the preceding phase of the project using data from the Municipality of Amsterdam. Its results were used to categorise the following six Age Classes based on frequency rank (i.e., #6 scenarios): *Young-1* (<5 years, rank #4), *Young-2* (10-15, #2), *Middle-age-1* (40-45, #5), *Middle-age-2* (45-50, #3), *Old-1* (65-70, #1), and *Old-2* (75-80, #6). For these ID2 scenarios, a fixed tree spacing of 10 m was applied (municipality proposal for NCs).

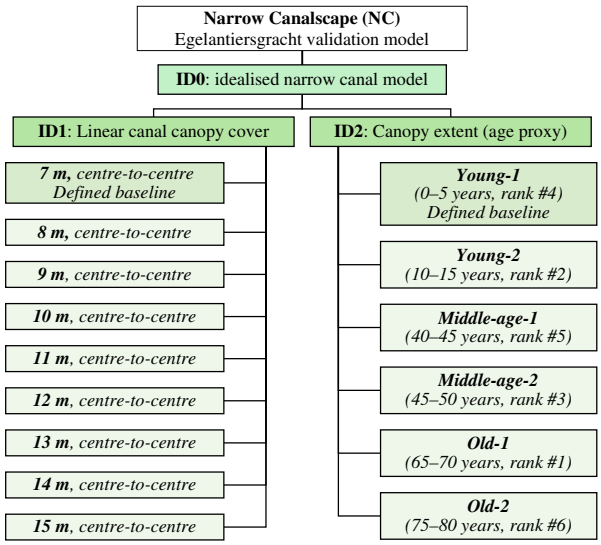


Figure 4. Tree integration scenario development.

2.3 Simulation and processing

Similar to validation (VAL) cases, each derived ID1 and ID2 scenario group was simulated using a horizontal and vertical resolution of 1 m to capture the microscale geometry of canal environments. The outputs included microclimatic variables such as T_a, V_a, direct shortwave radiation (SW↓), and T_{mrt}, as well as Physiological Equivalent Temperature (PET), the thermal comfort index widely discussed in outdoor heat-risk studies [14].

Post-processing was completed using a MATLAB workflow. Spatial and statistical analyses were performed to compare the two tree-integration scenario groups, focusing on changes in PET temperature and PET Categories, as well as Shading Fraction, as performance indicators of thermal comfort modification along the canals.

2.4 Reporting performance indicators

For consistent reporting across scenarios, three performance indicators are presented: changes in (1) Average PET, (2) PET Categories, and (3) Shading Fraction.

PET average and Categories

For each quay (i.e., two canal banks), PET is sampled at 1.5 m height between local time hours 12:00 and 18:00, and averaged per 1 m^2 voxel across this window, in accordance with *Standard Heat Stress Test* guidance [15]. The change in this mean PET value is expressed as a relative (Δ) reduction or increase when compared to a defined baseline to discuss performance.

The above average PET sampling is also classified into nine thermal sensation/stress classes following the widely used index (*Very cold → Extreme heat* [15–16]). The change in the spatial distribution of these Categories at 1.5 m height is again expressed as a difference (Δ) relative to a defined baseline to discuss performance.

Shading Fraction (SF)

ENVI-met outputs a *ShadowFlag* (i.e., atmospheric shading flag, 0/1); which is *True* (1) when ray-tracing determines that the potentially received Direct Shortwave Radiation (SW↓) at a voxel is lower than a threshold (≈5% of potentially received), owing to obstructions and/or transmissive shading (e.g., tree). Direct shortwave radiation (*QSWDirHorizontal*) is used to identify sunlit hours (i.e., values >2 $W \cdot m^{-2}$ at the cut level of 1.5 m above the quay level). The *ShadowFlag* is a binary diagnostic of direct-sun obstruction in the atmosphere grid; using it only during sunlit hours (i.e., 12:00 - 18:00) avoids counting the nighttime, while the SW↓ check is a pragmatic safeguard against low-sun or overcast threshold instances. Counting the number of sunlit hours with *ShadowFlag* = 1 for each voxel and dividing by total sunlit hours presents the Shaded Fraction (%). The change in this fraction for the quay surfaces at 1.5 m height, is expressed as a percentage point (Δ *pp*) difference relative to a defined baseline to discuss performance.

The processing of these performance indicators was achieved via a MATLAB workflow, using data extracted from ENVI-met's NetCDF output files, for the selected two quays and hours. A parity test compared PET values exported from *Panoply* (a cross-platform NetCDF dataviewer [17–18]), with those extracted by the MATLAB reader for 25-Aug at 12:00; with 600 matched grid-cells, maximum absolute difference of 5×10^{-5} °C, mean absolute difference of 2.5×10^{-5} °C, and RMSE of 2.9×10^{-5} °C. These results confirmed numerical equivalence to within machine precision for NetCDF fields to validate the extraction workflow, while the (Δ) differences relative to defined baselines were calculated subsequently in Excel.

The statistical analysis considered non-parametric statistics for the variables PET, PET Category, and Shaded Fraction. This was based on the data being scenario level aggregates, presenting non-normal distributions, and including ordinal and bounded variables (PET Category and Shaded Fraction). With ID1, linear regression quantifies PET sensitivity to a continuous control variable, with slopes, R^2, and *p*-values indicating the robustness and dominance of spacing effects (i.e., validity of sensitivity slope). With ID2, the Spearman's rank correlation (ρ) tests whether PET follows a consistent monotonic ordering, with *p*-values interpreted as indicators of trend robustness across the discrete levels. Across both ID1 and ID2 results, statistical significance thus seeks to confirm consistency, non-random behaviour, and supporting design-relevant conclusions, rather than generalisation beyond the simulated scenarios.

3 FINDINGS

This section presents the results for the validation (VAL) cases first, followed by the two tree-integration scenario groups simulated for a *warm* and *hot day*.

3.1 Validation results

The metrics used to evaluate the accuracy of the narrow canal model are listed in Table 4 for each VAL case, with the assessment prioritising Willmott's d.

Table 4: Validation (VAL) case results.

Validation Metrics		VAL 01	VAL 02	VAL 03	VAL 04	VAL 05	VAL 05a	VAL 05b	VAL 05c	VAL 05d
T_a	***d***	**0.88**	**0.89**	**0.88**	**0.88**	**0.88**	**0.88**	**0.89**	**0.88**	**0.89**
	RMSE	0.97	0.93	0.97	0.95	0.97	0.97	0.93	0.95	0.94
V_a	***d***	**0.55**	**0.55**	**0.24**	**0.27**	**0.72**	**0.72**	**0.72**	**0.72**	**0.72**
	RMSE	0.83	0.83	0.86	0.87	0.67	0.67	0.67	0.67	0.67
T_{mrt}	***d***	**0.55**	**0.54**	**0.54**	**0.54**	**0.55**	**0.55**	**0.55**	**0.54**	**0.54**
	RMSE	11.71	11.73	11.76	11.74	11.71	11.71	11.65	11.71	11.72

Results are presented in relation to the earlier mentioned simulation configuration options: (**a**) mean- *vs* median-based timestep aggregation; (**b**) wind smoothing options; and (**c**) priming / spin-up / warming-up period.

(a) When a single timestep aggregation method must be adopted across ENVI-met output variables for consistency, mean aggregation was preferred, as median aggregation substantially degraded V_a agreement ($d = 0.571$ *vs* 0.721; $RMSE = 1.019$ *vs* 0.669). This loss dominated cross-variable performance, whereas the improvements offered by median aggregation for T_a ($\Delta d = +0.003$; $\Delta RMSE = -0.053$), and T_{mrt} ($\Delta d = +0.005$; $\Delta RMSE = -0.033$), were modest.

(b) With the adopted mean-based aggregation, the *W2* wind-smoothing approach emerged as the optimal profile (from the *VAL05* family review). Its 16-hour implementation (i.e., case *VAL05b*), achieved the lowest composite score (4), ranking first for both V_a and T_{mrt}, as well as a near-optimal second for T_a.

(c) When nominally warmed (7-hour) simulations were compared with progressively warmed configurations (16, 24, and 48 hours), warming generally improved agreement for T_a and V_a under mean-based aggregation. However, these benefits saturated at moderate warming durations, with the 16-hour run having captured most of the improvement observed relative to the 7-hour run. For T_{mrt}, which is the primary driver of PET in outdoor environments [19–20], extended

warming-up beyond this level degraded agreement, with both 24- and 48-hour simulations performing marginally poorer than the 16-hour run.

In summary, the validation cases studied highlighted the optimal way forward by using 30-minute mean aggregation of ENV-met output values to compliment standard forcing input mean aggregation; signal smoothing applied to maintain flow deviations within permissible WS and WD bounds; and using a moderate priming / warming-up duration. The ***VAL05b*** case was accordingly applied as the template for the tree-integration scenario assessments.

The validation studies were carried out for an average warm day in Amsterdam (25-August). However, a key objective of the project is to consider ever-increasing frequency of heatwave conditions when pedestrian heat stress mitigation is a significant necessity in inner-city locations like Amsterdam's UNESCO zone. The weather file *W3* was processed to address this requirement, with 01-July selected for representing the warmest day of 2025 (Schiphol Station 240; see Table 1 and Table 3).

3.2 Tree integration results

This section presents trends and key observations for the two narrow canal scenario groups: (ID1) linear canal-bank tree spacing variation (7→15 m); and (ID2) trees by Age Class (canopy extent proxy) variation (Figure 4). The results are presented for both the *warm* and *hot* day-types. All differences (Δ) are interpreted relative to the defined baseline reference in each group. For ID1: this is the 7 m spacing, representing the traditional tree-spacing minimum; while for ID2 this is the *Young-1* Age Class, representing the lowest contributing tree canopy.

Notably, while the mean PET Category index was evaluated for both ID1 and ID2, it is not presented as a primary outcome in this narrow canal assessment, as the averaged Category class remained effectively unchanged across the scenarios (circa Category 3 on the *warm day* and Category 5 on the *hot day*). As a result, the PET Category metric provided limited additional insight, beyond continuous PET and Shaded Fraction results.

ID1: Linear tree spacing effect

Increasing elm spacing consistently increases PET and decreases Shaded Fraction (monotonic response). PET increases between 0.17-0.24 °C of added per meter trunk centre-to-centre spacing, while Shaded Fraction decreases between 0.99-1.87 percentage points (*pp*) per meter for both *hot* and *warm days* (see Table 5). PET sensitivity (°C increase) is larger on the *hot day* (~40% higher than the *warm day*), while the Shaded Fraction drop (percentage points) is larger on the *warm day*. PET and Shaded Fraction coupling (Spearman ρ) highlights shade loss as a strong monotonic driver of PET increase.

The top bank typically retains higher Shaded Fractions and smaller PET penalties than the bottom bank as spacing widens. Given the orientation, this implies the design limits to be governed by the bottom bank.

Table 5. ID1 endpoint effects; and PET and SF sensitivity

Day	PET 7 m (°C)	PET 15 m (°C)	ΔPET (°C)	SF 7 m (%)	SF 15 m (%)	Δ SF (*pp*)
Warm day	23.37	24.69	1.33	59.4	44.27	-15.13
Hot day	35.48	37.27	1.79	46.92	38.12	-8.8

Note: Δ relative 7 m spacing.

PET & SF sensitivity to spacing and coupling (both banks):

	Day	Slope (°C/m)	R^2	*p*-value
PET	*Warm day*	0.170 °C/m	0.99	<0.001
	Hot day	0.236 °C/m	0.99	<0.001
SF	*Warm day*	-1.87 *pp*/m	0.87	<0.01
	Hot day	-0.99 *pp*/m	0.79	<0.01

	Day	Zone	ρ	*p*-value
PET *vs* SF	*Warm day*	Both banks	-0.94	<0.001
	Hot day	Both banks	-0.91	<0.001

ID2: Tree canopy extent effect

For both banks/quays, PET reductions of 2-3.7 °C are presented by *Mid-Age-1* and *Old-1 Age* Classes relative to *Young-1*. Larger canopy Classes in general (Mid-age → Old), reduced PET in all canal and day combinations. The mature *Old-1 Class* was the best performer and consistently presented the lowest PET results across groups. The strongest canopy benefit occurred at the bottom bank or west-facing quay, on the *hot day* (Table 6).

Table 6. PET and SF relative to Young-1 (both banks).

Day	Age Class	PET (°C)	ΔPET (°C)	SF (%)	Δ SF (*pp*)
Warm	***Young-1***	27.03	0.00	43.31	0.00
Warm	*Mid-Age1*	24.85	-2.18	43.44	0.13
Warm	*Old-1*	23.77	-3.25	49.1	5.79
Hot	***Young-1***	39.90	0.00	36.99	0.00
Hot	*Mid-Age1*	37.47	-2.44	36.99	0.00
Hot	*Old-1*	36.16	-3.74	40.17	3.17

Note: Δ relative to *Young-1* Age Class.

Monotonic PET trend across Age Class (Spearman):

Quay Zone	*Warm day* ρ	*p*-value	*Hot day* ρ	*p*-value
Both banks	-0.71	< 0.05	-0.65	< 0.05
Bottom bank	-0.82	< 0.01	-0.89	< 0.01

Note: Top bank showed a weaker monotonic trend ($\rho \approx$ -0.5 to -0.6), reflecting smaller PET gradients and minor rank variations across intermediate Age Classes.

Notably, the Shaded Fraction changed only modestly, while some Age Class variants presented notable PET reductions without proportional Shaded Fraction gains. This implies influence from other processes contributing to these PET reductions.

4 DISCUSSION

4.1 Workflow validation

It is important that any numerical-based simulation study utilises appropriate and most approximate static and dynamic boundary conditions. It is also essential to

validate these boundary conditions prior to developing idealised scenarios. In this way the idealising is derived from a validated condition, which was the purpose of the first phase of this study, the results of which then defined the workflow for assessing tree-integration scenarios.

The dynamic inputs represented by weather variables are critical determinants of approximation relevance and consistency. While KNMI raw data offered good validation for T_a and T_{mrt} approximation, it was difficult to complete error-free simulation runs using this data, as it often led to numerical instabilities and blow-up (notably occurring with longer simulation durations). In such instances manual editing of WS and WD datapoints would be necessary to circumvent such failures. A signal-smoothing approach in contrast offers a more systematic approach to refining the temporal resolution of WS and WD, which then enables ENVI-met to more reliably generate and propagate the associated flow regimes over the requested simulation periods. It is important to note that within this signal-smoothing workflow, the validated outcome concerns the enhancement of WS and WD granularity. For any given signal window, the smoothing parameters must be individually tuned to achieve sufficient noise reduction without introducing distortions. Consequently, the smoothing settings are not static but vary for each window of interest (25 Aug or 01 July), as the characteristics of the raw signal differ across the full dataset.

Typical ENVI-met workflows have recommended simulation starting time to be set at or before sunrise, and use 24-48 hour spin-up / priming / warming-up [21]. This study highlighted that such longer warm-up durations to not provide additional numerical benefit for T_{mrt}, while moderate warming of 16-hours presented a good balance between T_a, V_a, and T_{mrt} agreement. When PET-relevant accuracy is prioritised as in this study, this presents an optimal approach. It is particularly pertinent given the parametric assessments considered, and the computation and resource efficiency required.

The reporting performance indicators used in this study had been selected to address the broader reporting consistency of the project, and support the discussion of relatable microclimate improvement options across multiple scenarios and iterative design-based workflows. PET is a well-acknowledged heat stress indicator as it reasonably reflects how people experience heat in outdoor environments. It captures the combined effects of sun/shade, WS/WD, humidity, and T_a, and is strongly correlated to comfort, health, and outdoor activity. Heat stress occurs at around 23°C, with higher values correlating with increased heat-related morbidity and mortality. Cross-sectional observations however are not necessarily indicative of structurally warmer conditions that generate sustained stress and long-term impact. To acknowledge that at a given location it can vary significantly due to dynamic sun/shadow patterns, the *Klimaateffectatlas* [15] heat stress maps had considered an averaged PET between 12:00 and 18:00 to identify structurally warmer at-risk conditions. Locations that show heat stress over a longer period during the day have therefore been rated higher in their revised PET-Categorisation. This in turn presents a more representative indicator of persistent problem locations, where spatial heat adaptations can make significant long-term mitigation contributions.

This assessment time window however extends to include late evening hours between 16:00 and 18:00, when the west-facing quay is disproportionally solar-loaded. While this disproportionality is acknowledged, including these evening hours is necessary to account for the urban heat island effect that gains potency towards the evening. Encompassing this peaking influence is essential as the heat dosage that pedestrians receive during this period is enhanced, with the shortwave radiation load depletion being compensated by the gradually increasing longwave radiation load emitted by warmed-up quay-canyon materials and the canal waterbody [2].

It is significant to recognise the limitations of the PET Category metric, which represents an ordinal simplification of the continuous PET scale. Meaningful improvements or penalties in PET Category require substantial shifts in PET values. In this study, most results remained closer to Category 3 (*Slight Heat Stress*) on the *warm day* and Category 5 (*Strong Heat Stress*) on the *hot day*. On the *hot day* in particular, both ID1 and ID2 results were closer to Category 5, providing no capacity for the metric to distinguish between scenarios. This results in a ceiling effect, where even changes in PET >1-3°C are not reflected in the Categorical reporting. While PET Category can be useful for communicating general improvements or penalties in thermal conditions to lay audiences, it is better suited to discrete, peak-hour assessments where category shifts are more likely to occur. In contrast, it is less effective for spatiotemporally averaged analyses, where such shifts are often absent or obscured.

4.2 ID1: Linear tree spacing influence

Asymmetric solar exposure was represented by the top bank typically exhibiting higher Shaded Fractions than the bottom bank at the same spacing, where bottom bank Shaded Fractions had very low values at larger spacings. This implied reduced effectiveness of linear tree cover for the more sun-exposed quay. For canals with pedestrianised quays on either side, the spacing implemented at the most exposed quayside has a determining influence. The significance of this was greater for the *hot day* than the *warm day* in terms of PET, while Shaded Fraction decreases were larger on the *warm day*.

On average warm days, overall heat stress is lower and changes in PET are less pronounced, although shade becomes a more significant comfort factor. Increasing tree spacing can as a result lead to noticeable reductions in the fraction of shaded area. This general sensitivity to shade loss in narrow canal environments however is moderated by their compact geometry. Spatial enclosure, overlapping canopy shade effects, and cross-canal shading maintain a relatively high baseline Shaded Fraction,

meaning that even as tree spacing increases, reductions in shade are smaller and more gradual. As a result, pedestrian comfort on average warm days remains well-supported, even under suboptimal tree spacing.

On hot days, small changes in tree spacing can strongly influence thermal stress, making spacing particularly critical under extreme conditions. However, PET sensitivity to spacing in narrow canals is again moderated by their geometry. The limited sky-view, greater enclosure, and reduced direct solar penetration prevent extreme heat build-up, resulting in a dampened PET response even as spacing increases. Although wider tree spacing still leads to reduced shade, the rate of decline is slower, supported again by overlapping canopies, adjacent building shade, and cross-canyon enclosure preserving shaded areas. As a result, linear tree planting in narrow canals remains relatively tolerant of wider spacing, maintaining cooling and comfort benefits even on extreme hot days.

In narrow canals, the proximity of the two banks allows mature tree shade and cooling effects from one side to influence the opposite, causing the canal canyon to function as a connected microclimate rather than as two independent quays. This promotes a more even distribution of cooling benefits, even when solar exposure differs between banks, with trees on the less exposed side moderating heat stress on the sunnier quay. Nevertheless, overall cooling performance is still most sensitive to tree spacing along the most solar-exposed quayside. From a design perspective, this means prioritising adequate tree spacing on the exposed quay to mitigate extreme heat, while recognising that on milder days pedestrian comfort is more closely tied to the continuity of shade rather than to large changes in heat stress.

4.3 ID2: Age Class (canopy extent influence)

ID2 scenario group results indicated the increasing of canopy extents as proxied by Age Class, to reduce PET and generally increase Shaded Fraction relative to the *Young-1* baseline (an elm <5 years of age that offers viable canopy cover). The largest PET reductions were consistently associated with the *Old-1* Age Class, which represents mature elms and canopy extents expected from a healthy tree representative of central Amsterdam.

Notably, the Shaded Fraction response was not always proportional to PET reductions, suggesting that processes beyond binary hour-count shading has influence. The processes that contribute to this include shading intensity under transmissive canopies, longwave radiation attenuation, reduced within canopy T_{mrt}, and evapotranspiration. In essence, canopy biophysical processes, and not only shade duration, influences PET improvement.

The weak association between Shaded Fraction and PET may also be partly attributed to the analysis spatial resolution. The ENVI-met 1 m^3 voxel resolution means that the binary hour-count approach only acknowledges and reports substantial enhancements in canopy cover shading. As a result, it underestimates shading associated cooling to present a conservative assessment.

This conservative shading associated cooling assessment is justified, given that it assumes consistent healthy tree cover without any canopy voiding, which is an ideal state of tree canopy shading. This idealised assessment must also be considered in relation to the general limitations of tree cover. The results highlighted older, more mature canopies to present the maximum benefit of tree cover associated cooling contributions, which is a state that is manifested after many years of healthy growth. Thus, the magnitude of beneficial results discussed here are only experienced after many years of well-supported tree growth and maintenance, which is not always realised in densely constructed cities. Caution must also be exercised when interpreting performance over prolonged heat stress conditions. Trees like all plant life suffer from prolonged heat stress related growth inhibition, physiological disturbance, and eventual canopy attrition. However, their perennial woody structure enables acclimation through antioxidant systems and osmotic adjustments that makes them more resilient than herbaceous species [22]. From a design perspective, urban trees therefore represent the most robust passive, nature-based intervention for enhancing the thermal environment of canal quays.

4.4 Implications for heritage canals

A central objective of urban tree enhancement programmes is to ensure that trees achieve their expected mature canopy extents as efficiently as possible. The rate at which this occurs is governed by site-specific environmental conditions and species selection. In urban canal environments, trees are subject to numerous constraints, which are further intensified in narrow canals with complex heritage, structural, and logistical limitations.

In Amsterdam, decades of applied practice have led to a strategic prioritisation of elms (*Ulmus* spp.), as one of the most resilient and adapted species for brackish canal environments. However, preceding project work had demonstrated that elms do not consistently attain their expected mature canopy size. This underperformance has been attributed primarily to insufficient volumes of rootable soil capable of sustaining healthy long-term growth.

Tree spacing is therefore a critical design parameter, as the achievement of mature canopy cover is intrinsically linked to growth rates, tree health, and the availability of rootable soil volume. In canal settings, subsurface conditions are highly constrained by the brackish water table, quay wall constructions, and heavily compacted subsoil resulting from vehicular traffic. As a result, opportunities for root development are largely restricted to lateral directions, where roots must compete both with neighbouring trees and subsurface infrastructure and logistical functions associated with quay use.

These constraints generate increasing pressure to adopt wider tree spacings, and in some instances, to introduce intentional gaps within linear planting proposals. The findings of this study demonstrate that wider spacing regimes intended to reduce root competition and ease

limitations in available soil volume, can remain effective in narrow canals without substantially compromising canopy cover or its associated thermal comfort and heat stress mitigation benefits. Optimal tree spacing can therefore be negotiated as a balance between ecological performance and the practical requirements imposed by logistical and infrastructural constraints. Furthermore, where gaps in tree cover are unavoidable to accommodate such constraints, the solar exposure prioritisation discussed earlier suggests that these should preferentially be located along the least exposed side of the quay to minimise adverse microclimatic impacts.

5 CONCLUSION

This conference paper presented scenario-based simulation results to justify the enhancement of green infrastructure provision along restored and enhanced quays, with particular emphasis and validation of the inclusion of elm tree arrangements to enhance pedestrian comfort, as well as mitigate heat stress during warmer periods.

In outdoor environments, Physiological Equivalent Temperature (PET) is most sensitive to mean radiant temperature (T_{mrt}), with reductions achieved through shading or geometric modification typically delivering the largest improvements. With the simulation validation datasets, T_{mrt} agreement was accordingly prioritised. The 16-hour mean-based, Savitzky-Golay smoothed scenario returned the highest T_{mrt} agreement among the primed/warmed configurations, making it the most appropriate approach for the subsequent PET-based simulation assessment objective of the parametric study.

With the succeeding tree-integration scenario groups, ID1 is best described as a pure shading experiment (i.e., geometry), while ID2 described a canopy-process modification experiment (i.e., geometry and biophysical processes). ID1 spacing effects dominated radiative control of PET; increased spacing reducing canopy overlap and direct shortwave attenuation, thereby increasing mean radiant temperature and PET (0.17-0.24 °C per metre of added spacing). PET sensitivity to spacing was stronger under *hot day* conditions, consistent with higher background radiative loads (as well as the higher solar altitude in July). Bank/quay asymmetry was highlighted with the bottom bank more exposed for the study's given North-South orientation. In general terms the spacing design driver was thus the relatively more exposed quay of the canal canyon. ID2 Age-class effects exceeded binary shade metrics, with PET reductions occurring even with limited change in Shaded Fraction, implying the relevance of canopy transmissivity, longwave exchange, and evapotranspiration contributions.

In summary, the dominant PET driver of ID1 was radiative exposure (geometry), while with ID2 this included radiative, evapotranspiration, and canopy microclimate influences. In narrow canals, linear single row tree planting remains structurally effective, with intended performance not collapsing rapidly when spacing is increased. This makes such canals more resilient to design constraints and planting limitations that demand wider spacing. In essence, narrow canal geometries stabilise tree canopy benefits, making pedestrian comfort less sensitive to exposure differences and spacing choices.

The findings of this study provide actionable insights for municipalities and designers aiming to integrate nature-based solutions, particularly trees, into historic urban canal environments. The next phase of the project will expand the analysis to include the second canal typology (wide bed), as well as future-proofing assessments for both canal configurations to offer climate-resilient and functionally effective urban environments.

6 ACKNOWLEDGEMENTS

The work described is part of the *Multifunctional Quay Wall* project, funded by the Dutch National Growth Fund (NGF), under the *Future-proof Living Environment* programme, and facilitated by the AMS Institute.

7 REFERENCES

1. K. R. Gunawardena, Heat vulnerability: risk to health and wellbeing in the built environment, University of Cambridge, 2015.
2. K. Gunawardena, Fundamentals of Urban Heat Islands: Concise guide for architects and urban planners, University of Cambridge, 2018.
3. L. Kleerekoper, M. Van Esch, & T. B. Salcedo, How to make a city climate-proof: Addressing the urban heat island effect. *Planning for Climate Change: A Reader in Green Infrastructure and Sustainable Design for Resilient Cities*, 64 (2018) 250–262.
4. K. R. Gunawardena & T. Kershaw, Green and blue-space significance to urban heat island mitigation. In S. Emmit, & K. Adeyeye,eds., *Integrated Design International Conference (ID@50)* (Bath: University of Bath, 2016), pp. 1–15.
5. M. Bruse, ENVI-met: A holistic microclimate model. *ENVI-met Technical Documentation*, (1999).
6. E. Chatzinikolaou, C. Chalkias, & E. Dimopoulou, Urban microclimate improvement using ENVI-MET climate model. *International Archives of the Photogrammetry, Remote Sensing and Spatial Information Sciences - ISPRS Archives* (2018), pp. 69–76.
7. K. Gunawardena, Methodologies for assessing urban microclimates. *University of Cambridge, Department of Architecture, PhD Symposium* (Cambridge: University of Cambridge, 2018), pp. 1–20.
8. Z. Liu, K. Y. Cheng, T. Sinsel, H. Simon, C. Y. Jim, T. E. Morakinyo, Y. He, S. Yin, W. Ouyang, Y. Shi, & E. Ng, Modeling microclimatic effects of trees and green roofs/façades in ENVI-met: Sensitivity tests and proposed model library. *Building and Environment*, 244 (2023).
9. R. van der Velde, M. van Esch, D. Maiullari, & M. Pouderoijen, Cool Tree Architecture and Measurement Protocols. *12th International Conference on Urban Climate (ICUC12)* (Rotterdam, The Netherlands, The Netherlands, 2025).

10. A. Savitzky & M. J. E. Golay, Smoothing and Differentiation of Data by Simplified Least Squares Procedures. *Analytical Chemistry*, 36 (1964) 1627–1639.
11. K. R. Gunawardena, Wind signal smoothing: in EnergyPlus (EPW) or EnviMET (csv) weather files. (2025) 1–5.
12. K. R. Gunawardena, Agreement metrics calculator. (2026) 1–6.
13. P. J. Crank, A. Middel, P. Coseo, & D. J. Sailor, Microclimate impacts of neighborhood redesign in a desert community using ENVI-met and MaRTy. *Urban Climate*, 52 (2023) 101702.
14. J. Fischereit & K. H. Schlünzen, Discussion on thermal comfort indices. *International Journal of Biometeorology*, (2018).
15. T. de Nijs, P. Bosch, E. Brand, B. Heusinkveld, F. van der Hoeven, C. Jacobs, L. Klok, J. Kluck, A. Koekoek, S. Koopmans, K. van Nieuwaal, R. Ronda, & G. Steeneveld, Ontwikkeling Standaard Stresstest Hitte. (2019) 1–127.
16. A. S. Nouri, A. Lopes, J. P. Costa, & A. Matzarakis, Confronting potential future augmentations of the physiologically equivalent temperature through public space design: The case of Rossio, Lisbon. *Sustainable Cities and Society*, 37 (2018) 7–25.
17. NASA GISS, Panoply 5: netCDF, HDF and GRIB Data Viewer. (2026).
18. K. R. Gunawardena, ENVI-met NetCDF output data extractor. (2026) 1–4.
19. H. Lee & H. Mayer, Validation of the mean radiant temperature simulated by the RayMan software in urban environments. *International Journal of Biometeorology*, 60 (2016) 1775–1785.
20. S. Chen, N. H. Wong, C. Cen, R. Xu, L. Xu, Z. Shen, Z. Wu, J. Fu, & Z. Yu, Quantifying key design factors for thermal comfort in underground space through global sensitivity analysis and machine learning. *Tunnelling and Underground Space Technology*, 169 (2026) 107282.
21. D. H. S. Duarte, P. Shinzato, C. S. Gusson, & M. M. Brizotti, The impact of vegetation on urban microclimate to counterbalance built density in a subtropical changing climate. *Urban Climate*, 14 (2015) 224–239.
22. C. Zhou, S. Wu, C. Li, W. Quan, & A. Wang, Response Mechanisms of Woody Plants to High-Temperature Stress. *Plants*, 12 (2023) 3643.